

DYNAMIC MODEL OF THE INTERNAL PRESSURE IN A SOLID PROPELLANT ROCKET MOTOR

Saulo Gómez

Instituto Tecnológico de Aeronáutica
 sagomez@unal.edu.co

Hernán Cerón

Universidade de São Paulo
 hernan@sc.usp.br

Jhonathan Murcia

FU. Los Libertadores
 jomurciap@libertadores.edu.co

Abstract. *The internal pressure of the combustion chamber in a solid propellant rocket motor is a function of the physical and thermochemical properties of the used propellant, as well as the internal geometric configuration. This document presents an algorithm based on the finite difference method which is formulated to predict the comportment of the pressure during the fast combustion of the propellant grain, with a motor design and a type of propellant previously established. Two cases are compared and analyzed, A) cylindrical grain and radial burning, and B) cylindrical grain and longitudinal burning. Also, performance from different propellants materials can be compared with this model. Finally, the thrust-time curve is obtained from the calculated pressure and the equations for isentropic flow in nozzle, which is useful to determine the viability of each configuration in a given mission.*

Keywords: *finite difference, solid propellant, combustion chamber*

1. INTRODUCTION

The combustion process takes place inside the chamber in a rocket motor; it generates gases at high pressure and temperature that are then accelerated into a nozzle to supersonic speeds. Exhaust gases provide to the rocket of its thrust, according to the moment conservation principle (Sutton, 2010). If the elements necessary for the combustion, fuel-oxidant, are contained within the same molecule in a solid structure, the propellant is called a solid homogeneous propellant (Hill, et al., 1992).

In accordance with the cross section of the propellant and the burning direction, there are two basic types of solid propellants, internal (radial) and end (longitudinal) burning. They are illustrated in the Figure 1.

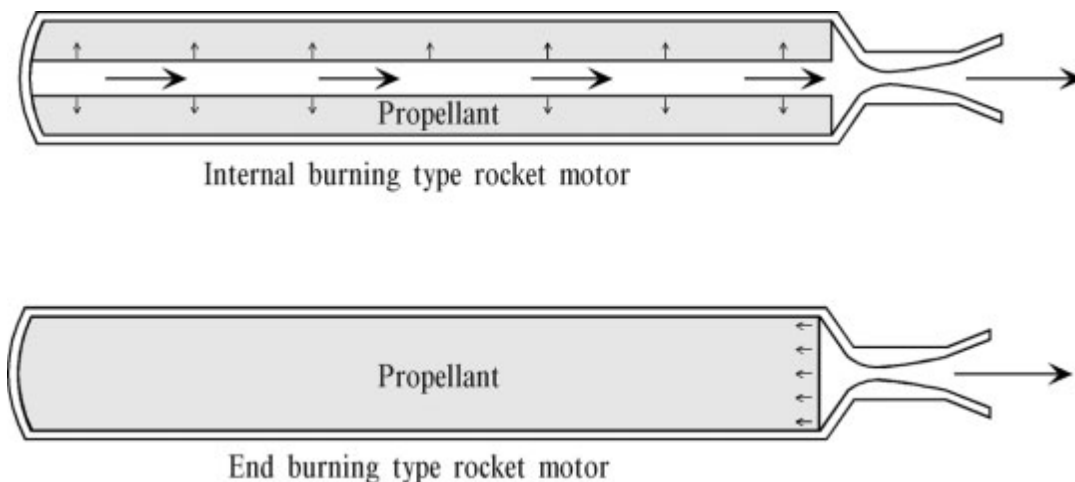


Figure 1. Types of burning in solid propellants (Kubota, 2007)

The pressure in the combustion chamber will be the result of the mass balance between the exhausted flow by the nozzle and the generated gases by the reactive surface.

To find a solution explicit for the pressure chamber is possible in an analytical way when the burning is radial, but not in the longitudinal case. This paper presents the development of a numerical solution for the end burning based on finite differences.

The design of a rocket engine proposed for the Sounding Rocket Project of the FU. Los Libertadores in Bogotá is used as application example. The selected propellant is double-base, whose physicochemical features and of the combustion gases are inputs of the algorithm. With the calculated pressure on the time and the relations for isentropic-compressible flow, the given thrust can be evaluated. Finally, numerical results are compared and analyzed.

2. ANALYTICAL VIEW

The mass balance equation in a rocket motor is presented by Hill as:

$$\frac{V(r)}{R_g T_0} \frac{dP_0}{dt} = A_b r (\delta_p - \delta_0) - c A_c P_0 \quad (1)$$

Where,

V : Chamber volume

R_g : Constant for ideal gas model

T_0 : Flame temperature

P_0 : Chamber pressure

t : Time

A_b : Area of burning surface

r : Burning rate

δ_p : Solid propellant density

δ_0 : Combustion products density

A_c : Critical area of the nozzle

c is a constant, function of the properties of the combustion products:

$$c = \sqrt{\frac{\gamma}{R_g T_0} \left(\frac{2}{\gamma+1}\right)^{\frac{\gamma+1}{\gamma-1}}} \quad (2)$$

γ : Specific heat ratio

The burning rate, r , is given by the Vieilley law (Kubota, 2007):

$$r = a P_0^n \quad (3)$$

a and n are empirical constants that depend of the propellant composition and the initial temperature before combustion. The exponent n defines if the combustion is stable or not as is indicated in the Figure 2.

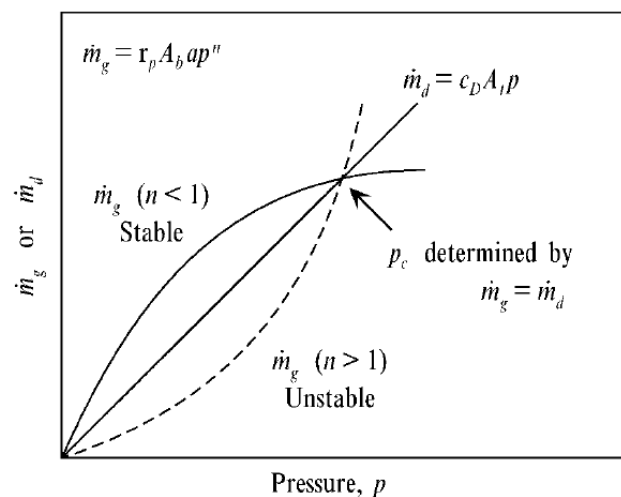


Figure 2. Stability argument for solid propellant combustion (Kubota, 2007)

End burning is illustrated in the Figure 3. The balance equation is applied in this case doing the following considerations: density of the combustion gases, δ_0 , is negligible; the burning surface, A_b , and the chamber volume, V_0 , remain constant.

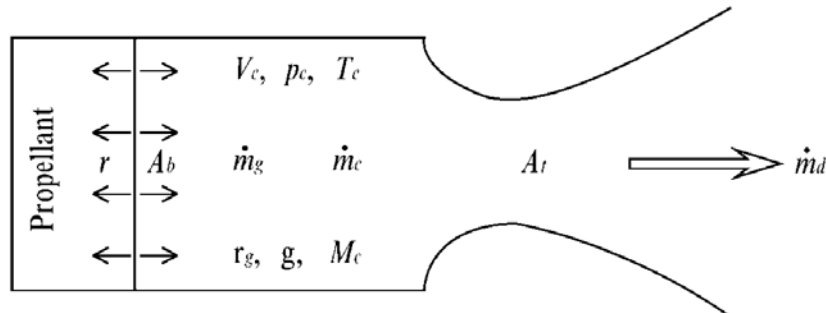


Figure 3. Mass balance for end burning (Kubota, 2007)

Now the balance equation can be rewrite in the form:

$$\frac{dP_0}{dt} + K_1 P_0 = K_2 P_0^n \quad (4)$$

If, $n \neq 0$ or 1 , Eq. (4) is named Bernoulli equation (Ross, 1984), it can be reduced to a linear equation by an appropriate variable change:

$$Q = P_0^{1-n} \quad (5)$$

Then, Eq. (4) transforms into a linear equation:

$$\frac{dQ}{dt} + (1-n)K_1 Q = (1-n)K_2 \quad (6)$$

Kubota solves P_0 as:

$$P_0(t) = \left[\frac{a\delta_p A_b}{cA_c} + \left(P_a^{1-n} - \frac{a\delta_p A_b}{cA_c} \right) e^{\frac{(n-1)R_g T_0 c A_c t}{V_0}} \right]^{\frac{1}{1-n}} \quad (7)$$

P_a is the initial chamber pressure or the local atmospheric pressure where the motor operates.

Equation (7) allows to obtain the characteristic time, τ :

$$\tau = \frac{V_0}{(1-n)A_t R_g T_0 c} \quad (8)$$

The steady state is reached when $t > 5\tau$.

The previous suppositions are invalid for internal burning. Here, V_0 and A_b should be expressed by:

$$V_0 = V_i + L_p \pi \left(\frac{\phi_1}{2} + \int_0^t r_{(P_0)} dt \right)^2 \quad (9)$$

And:

$$A_b = 2\pi L_p \left(\frac{\phi_1}{2} + \int_0^t r_{(P_0)} dt \right) \quad (10)$$

The values of a and n are the same that the end burning.

The resultant balance equation for internal burning is nonlinear, an explicit answer for P_0 is impossible. The next section shows a numerical approach to solve the pressure chamber in this case.

3. NUMERICAL APPROACH FOR INTERNAL BURNING

If the pressure function, P_0 , is continuous and differentiable at the time interval $A-B$, Figure 4, an algorithm based on finite differences to solve P_0 can be implemented. The interval is divided in a finite number of sub-intervals with width Δt_j each one.

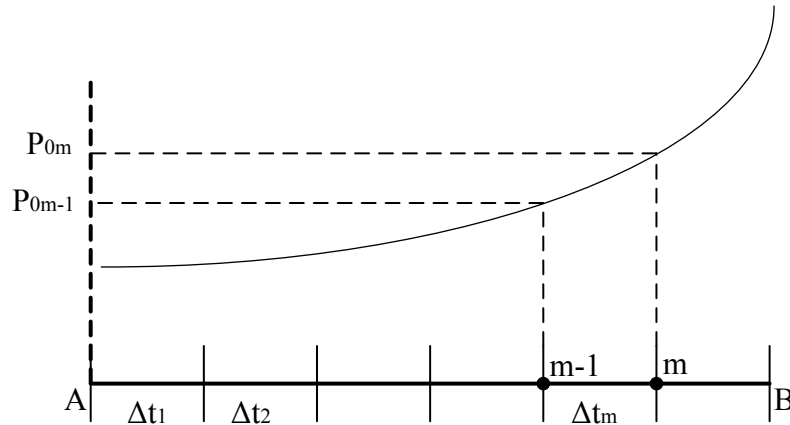


Figure 4. Numerical approach for the pressure chamber

Equation (11) is a discrete form of the balance equation in the domain shown on the Figure 4:

$$\frac{V_m + V_{i-1}}{2R_g T_0} \frac{(P_m - P_{m-1})}{\Delta t_m} = \frac{A_m + A_{m-1}}{2} a \left(\frac{P_m + P_{m-1}}{2} \right)^2 \delta_p - c A_c \left(\frac{P_m + P_{m-1}}{2} \right) \quad (11)$$

Also, V and A have a discrete form:

$$V_m = V_i + L_p \pi \left(\frac{\phi_1}{2} + \sum_{j=1}^m a \left(\frac{P_j + P_{j-1}}{2} \right)^n \Delta t_j \right)^2 \quad (12)$$

$$A_m = 2\pi L_p \left(\frac{\phi_1}{2} + \sum_{j=1}^m a \left(\frac{P_j + P_{j-1}}{2} \right)^n \Delta t_j \right) \quad (13)$$

Using the value of P_{m-1} and replacing the definitions of V_m and A_m in Eq. (11), a nonlinear equation for the implicit unknown P_m is obtained and can be resolved by any iterative method.

This approach is valid for end burning, if A_m is considered constant and V_m is write as:

$$V_m = V_i + \sum_{j=1}^m a \left(\frac{P_j + P_{j-1}}{2} \right)^n \Delta t_j \quad (14)$$

In both cases, the counting for P_m finishes when V_m reaches the chamber volume without propellant.

4. CASE STUDY

The motor design corresponds to the preliminary prototype of the sounding rocket *Libertador I*, which is currently been developed by the F.U. Libertadores in Bogotá (Murcia, et al., 2012). Its internal dimensions are presented in the Table 2.

A double base composition, whose main constituents are nitrocellulose (NC), nitroglycerin (NG) and diethyl phthalate (DEP), is selected as propellant. Combustion of a double base propellant produces high temperature and low molecular mass gases, leaving a smokeless signature. The distribution of its energetic components is near to stoichiometric balance. In addition, the burning rate is well described by the Vieille law, Figure 5.

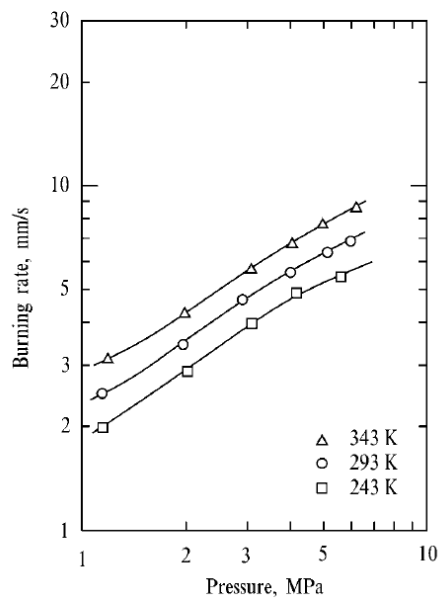


Figure 5. Burning rate curve of the selected double-base propellant

Composition and other characteristics of the selected propellant are shown in the Table 1.

Table 1. Characteristics of the selected propellant (Kubota, 2007).

Initial composition:	
NC	37.5%
NG	50.0%
DEP	12.5%
Combustion products by mol:	
CO	41.5%
CO ₂	11%
H ₂	13.4%
H ₂ O	22.2%
N ₂	11.9%
Other characteristics:	
δp [kg/m ³]	1530
T_o [K]	2557
R_g [J/kgK]	346
γ	1.24
n	0.7
a [mm/s.MPa ⁿ]	2
σ [1/K]	0.0038

To evaluate the performance of each burning type, two motors have been projected. Chambers dimensions not change. However, the burning area, A_b , is greater for internal burning. Therefore, nozzle dimensions are not the same. These differences are presented in the Table 2.

S. Gómez, H. Ceron and J. Murcia
Dynamic Model of the Internal Pressure in a Solid Propellant Rocket Motor

Table 2. Motor geometry configuration.

	End Burn.	Internal Burn.
Propellant length [mm]	900	900
Chamber diameter [mm]	64	64
Inner propellant diameter [mm]	-	27
Throat diameter [mm]	3	20
Exit diameter [mm]	10	40
Propellant mass [kg]	4.43	2.95

With the atmospheric pressure, $P_a = 101325$ Pa, algorithm inputs are completely defined for each case.

5. RESULTS

First, obtained results of the algorithm for end burning are presented and compared with the analytical model, Eq. (7). Consequently, precision of the numerical method can be quantified. Chamber pressure evaluated by these two methods is shown in the Figure 6.

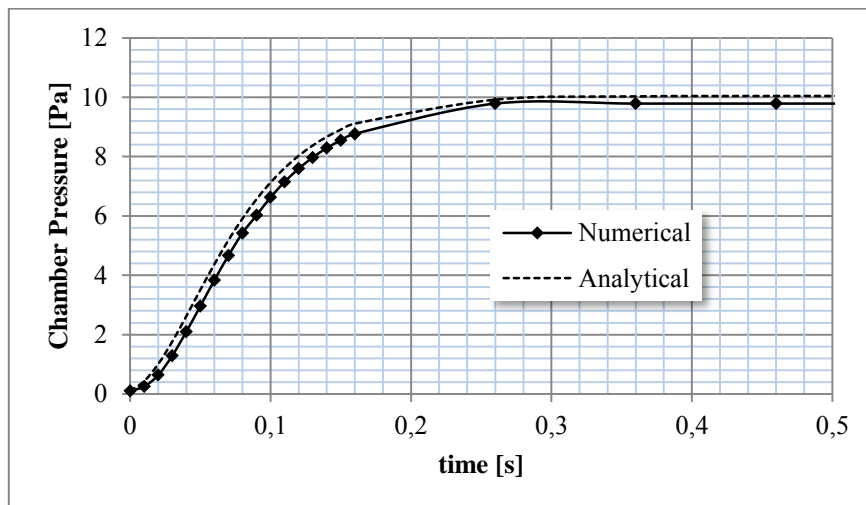


Figure 6. Chamber pressure for the end burning

The error for the steady pressure is 2.5%. The time to reach the steady pressure is determinate by Eq. (8): $5\tau \approx 246$ ms.

In spite of the high chamber pressure, the mass flow in the nozzle is 49.2 g/s, a low thrust: 11.8 kgF is obtained. The combustion is maintained during 91.5 s approximately.

Now, internal burning is examined. Chamber pressure and mass flow are represented by the plot in the Figure 7.

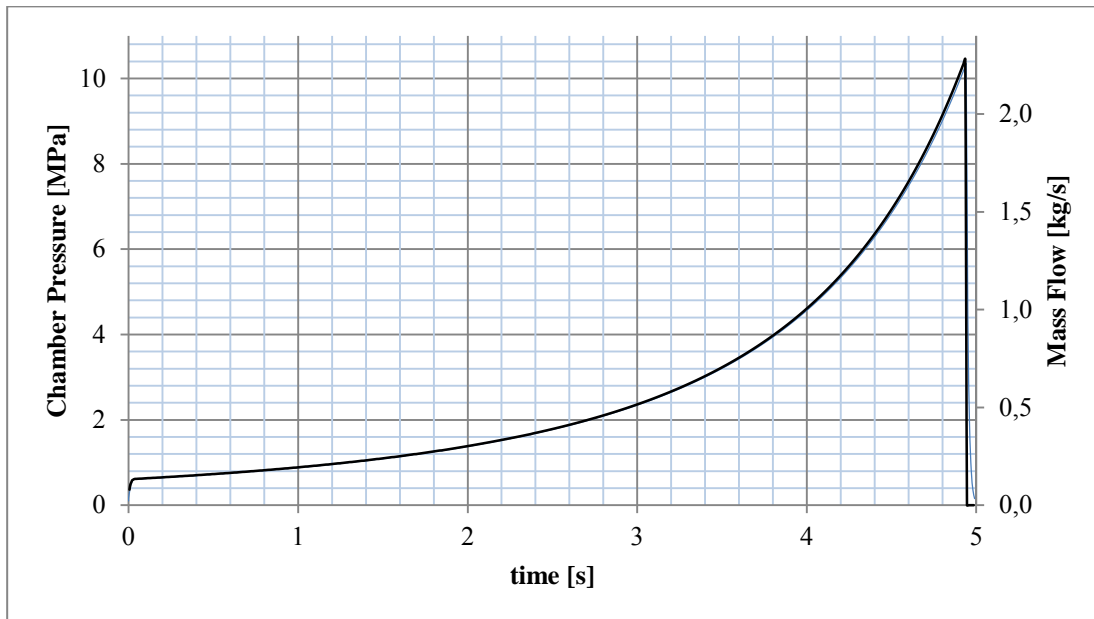


Figure 7. Chamber pressure for the internal burning.

Figure 7 indicates that internal burning provides an increasing pressure; this change is associated to the variation of the burning area. The highest pressure (≈ 10 MPa) should be the base to choose material and thickness of the wall chamber.

If the calculated pressure is considered in the relations for isentropic-compressible flow of nozzle (Sutton, 2010), to estimate the thrust and its comportment on the time is possible.

Figure 8 indicates the resultant thrust history for both burning types.

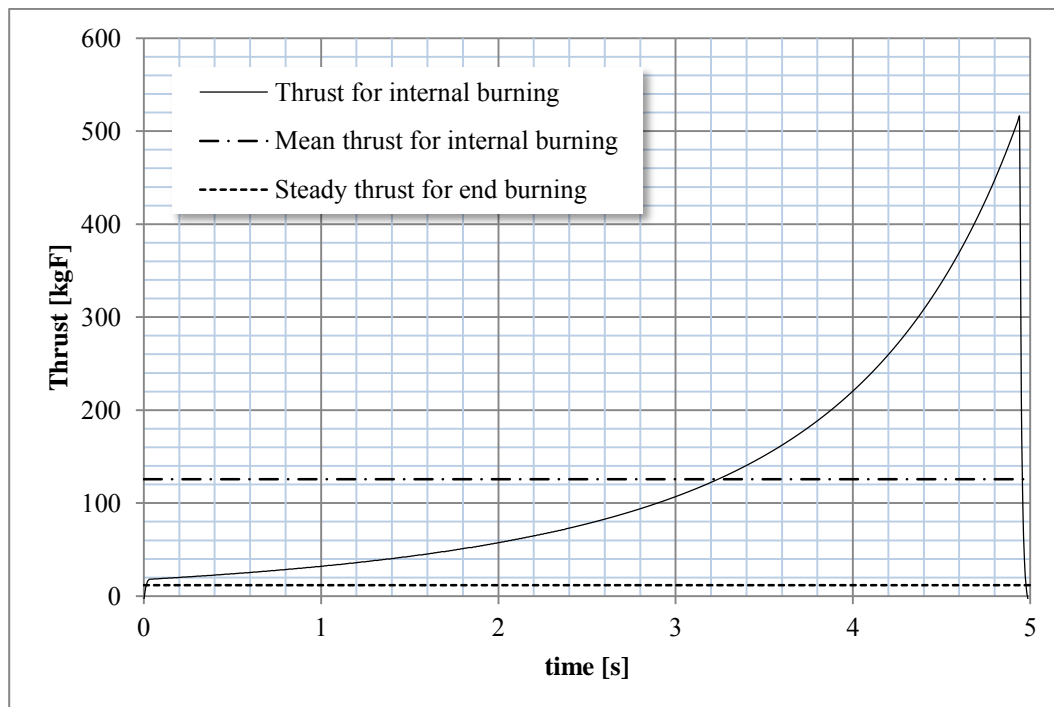


Figure 8. Given thrust by radial and end burning

The plot of the

Figure 8 allows estimate the trajectory of the rocket vehicle that uses the studied motor. The mean thrust is defined as:

$$F_m = \frac{\int_A^B F(t) dt}{B-A} \quad (15)$$

F_m is a characteristic value of the performance of the ensemble motor-propellant and can be used to evaluate different configurations. Also, F_m allows to quantify the total effect of the change of one or more variables. As a result, optimum values that maximize the magnitude of F_m can be funded. Table 3 shows estimated values for F_m and other parameters that are characteristic of the total process.

Table 3. General results.

	End Burn.	Internal Burn.
Mean thrust [kgF]	11.8	125.7
Combustion time [s]	91.5	5
Exit velocity [m/s]	2327	2059
Exit Mach	3.47	2.68
Specific Impulse [s]	237	210

The simulation shows that the mean thrust given by the configuration for internal burning is greater than ten times the steady thrust of the end burning configuration. For this reason internal burning type is preferred for atmospheric rockets.

6. CONCLUSIONS

The proposed method is a way to evaluate numerically the performance and other differences between types of burning as well as motor designs and propellant compositions.

For end burning type, numerical results offer enough precision, compared with the analytical model. For radial burning, the behavior described by the algorithm corresponds to qualitative descriptions of the provided force by this type.

High chamber pressure is obtained with the internal burning but the provided thrust is insufficient to propel atmospheric vehicles due to the low flow of exhausted gases. With internal burning, the motor give higher mean forces in short times.

Pressure and thrust plots that are obtained complement the accounting of other engineering aspects, as trajectory and wall of the combustion chamber.

If the parameters a and n in Eq. (3) are unknown, a test with internal burning can be conducted, measuring pressure or thrust and recording the burning rate. The last one is estimated as the ratio between the propellant length and the burn time. Chamber pressure is changed with the use of different throat diameter in the nozzle. With this information, a graph such as the one presented in the Figure 5 is rebuilt and the values a and n , characteristics of the propellant, are determinate. It can be used to predict the performance of the same propellant under radial burning.

Also, is possible to quantify the sensitivity of burning rate, σ , to initial propellant temperature, T_p , following the procedure described in the previous paragraph and adding the measurement of different values for T_p .

Laboratory tests are necessary to verify the proposed model. In principle, only is necessary to measure thrust and time, though verification of other variables as pressure and temperature is also desirable. In addition, obtained results of the simulation provide a criterion for selection of the respective measurement instruments.

7. REFERENCES

- Hill, P. and Peterson C., 1992. *Mechanics and Thermodynamics of Propulsion*. Addison Wesley, New York, 2nd edition.
 Kubota, N., 2007. *Propellants and Explosives*. Wiley-VCH, Weinheim, 2nd edition.
 Murcia, J.O., Cerón, H.D., Gómez, S.A., Pachón, S.N., 2012. "Diseño Conceptual, Preliminar y Análisis de la Trayectoria de Vuelo de un Cohete Sonda de Propelente Solido". In *Proceedings of the IV Congreso Internacional en Ciencia y Tecnología Aeroespacial - CICTA2012*. Bogotá, Colombia.
 Ross, S.L., 1984. *Diferential Equations*. Jhon Wiley and Sons, New York, 3rd edition.
 Sutton, G.P. and Biblarz O., 2010. *Rocket Propulsion Elements*. Jhon Wiley and Sons, New York, 8th edition.

8. RESPONSIBILITY NOTICE

The authors are the only responsible for the printed material included in this paper.